Design of an Affordable, Fully-Actuated Biomimetic Hand for Dexterous Teleoperation

Zhaoliang Wan[1], **Zida Zhou**[1 2], **Zehui Yang**[1], **Hao Ding**[1], **Senlin Yi**[1], **Zetong Bi**[1], **Hui Cheng**[1*]
Sun Yat-sen University [1] Orbot Ltd [2]

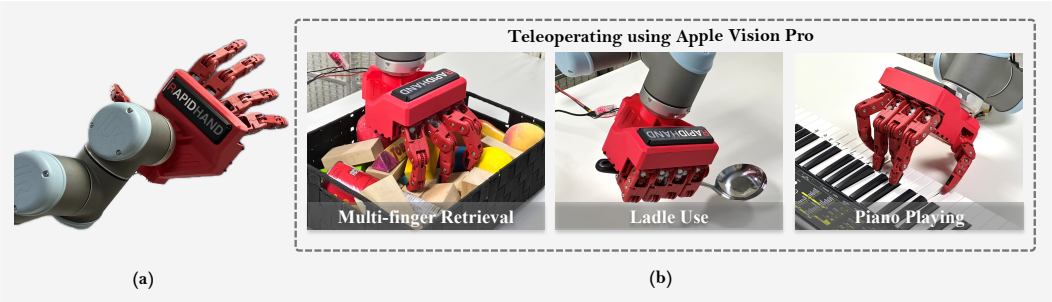

Figure 1: (a) RAPID Hand: a low-cost, fully-actuated, five-fingered hand. (b) Teleoperation of the RAPID Hand using Apple Vision Pro for three tasks.

Abstract: This paper addresses the scarcity of affordable, fully-actuated five-fingered hands for dexterous teleoperation, essential for collecting large-scale real-robot data in the "Learning from Demonstrations" paradigm. We introduce RAPID Hand, a low-cost, 20-degree-of-actuation (DoA) dexterous hand featuring a novel anthropomorphic actuation and transmission scheme with an optimized motor layout. It includes a universal phalangeal transmission for the non-thumb fingers and an omnidirectional thumb actuation mechanism. Prioritizing affordability, the hand uses 3D-printed parts for easy replacement and repair. We evaluate its performance through quantitative metrics and qualitative testing in three tasks: multi-finger retrieval, ladle handling, and human-like piano playing. The results show that the RAPID Hand's fully actuated 20-DoF design offers significant potential for dexterous teleoperation. The project will be open-sourced.

Keywords: Multi-fingered Hands, Dexterous Manipulation, Dexterous Teleoperation

1 Introduction

Dexterous manipulation [1, 2, 3, 4, 5] is a critical research area in both robotics and embodied AI. Recent advancements [6, 7, 8, 9, 10] have been largely driven by the collection of high-quality, real-world manipulation data combined with imitation learning. A key emerging trend is the use of low-cost teleoperation systems for data collection, which offer unique advantages. These systems enable precise demonstrations with smooth trajectories, facilitating the development of policies that generalize well to new environments and tasks.

Despite progress, two major challenges remain: the high cost of dexterous robotic hands and the difficulty of designing low-cost hands with high DoAs. Current affordable options [11, 12, 13, 14, 15] often have limited degrees of freedom (DoFs) or bulky designs, restricting their usefulness in tasks that require fine dexterity, such as tool use or piano playing.

[*] Correspondence to chengh9@mail.sysu.edu.cn.

8th Conference on Robot Learning (CoRL 2024), Munich, Germany.

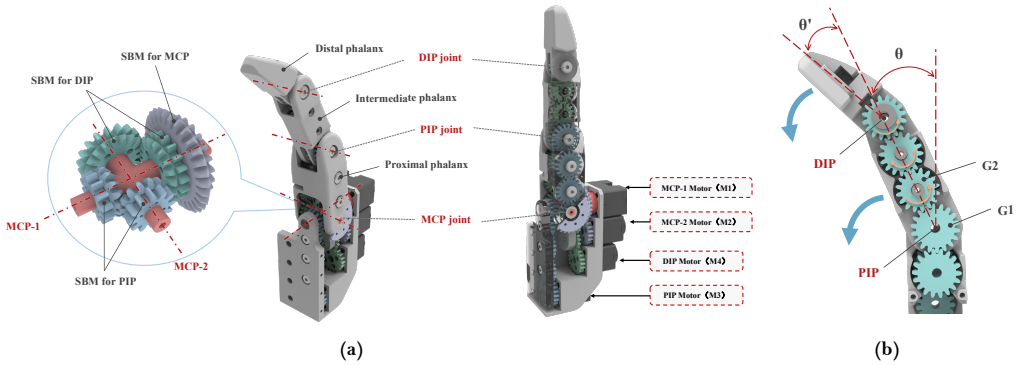

Figure 2: (a) **Multi-view of the index finger with universal phalangeal transmission scheme**. Red indicates MCP-1 transmission, purple for MCP-2, blue for PIP, and green for DIP. (b) **Effect of Joint Motion on Gear Transmission**.

To address these issues, we introduce the RAPID Hand, an affordable, fully actuated, biomimetic robotic hand with five fingers and 20 DoFs (Fig. 1 (a)). Designed for dexterous teleoperation, it uses off-the-shelf and 3D-printed components for easy repair and maintenance. The hand incorporates a **universal phalangeal transmission scheme** for non-thumb fingers and an **omnidirectional thumb actuation mechanism**, avoiding bulky finger designs seen in other systems.

We evaluate the RAPID Hand's performance through quantitative metrics like thumb opposability and manipulability ellipsoid volume, as well as qualitative tests on tasks such as multi-finger retrieval, ladle use, and human-like piano playing (Fig. 1 (b)). Results suggest that the RAPID Hand's 20-DoF design holds promise for dexterous teleoperation.

2 Design For Dexterity

2.1 Hand Kinematics

Since most household objects are designed for human hands, the RAPID Hand closely replicates human hand kinematics. As noted in [16], the human hand has five fingers, each with three joints. The thumb features interphalangeal (IP), metacarpophalangeal (MCP), and trapezoid-metacarpal (TM) joints, while the other fingers have distal (DIP), proximal (PIP), and MCP joints. The MCP and TM joints are ball joints, while the others are hinge joints. The RAPID Hand uses two DoFs to mimic these ball joints, resulting in a total of 20 DoFs. Achieving this in an affordable robotic hand is a significant design challenge.

2.2 Universal Phalangeal Transmission Scheme

The RAPID Hand introduces a **universal phalangeal transmission scheme** for the index, middle, ring, and pinky fingers, relocating motors to the palm to reduce finger size and weight. This design uses a gear-driven mechanism to ensure smooth, precise, and coordinated finger movements, as shown in Fig. 2. For the MCP joint, motor M1 controls abduction/adduction via a cross shaft, while M2 handles flexion/extension through a bevel gear mounted on the proximal phalanx. M3 drives the PIP joint, and M4 powers the DIP joint, each connected to their respective joints through dedicated gear sets.

One challenge is aligning motor output shafts with the MCP-1 axis while keeping the rotational axes of MCP-2, PIP, and DIP joints perpendicular. To address this, we designed the spur-bevel gear module (SBM), which integrates both gears into one unit, allowing a 90-degree shift in transmission direction while ensuring precise motion across all joints. As illustrated in Fig. 2 (b), the PIP and DIP joints share a planetary gear structure (G1, G2, and IP). When the PIP joint moves, G2 rotates relative to the IP, causing unintended DIP motion, even if M4 is inactive. Gear ratio analysis and careful transmission calculations are necessary to maintain independent control of each joint.

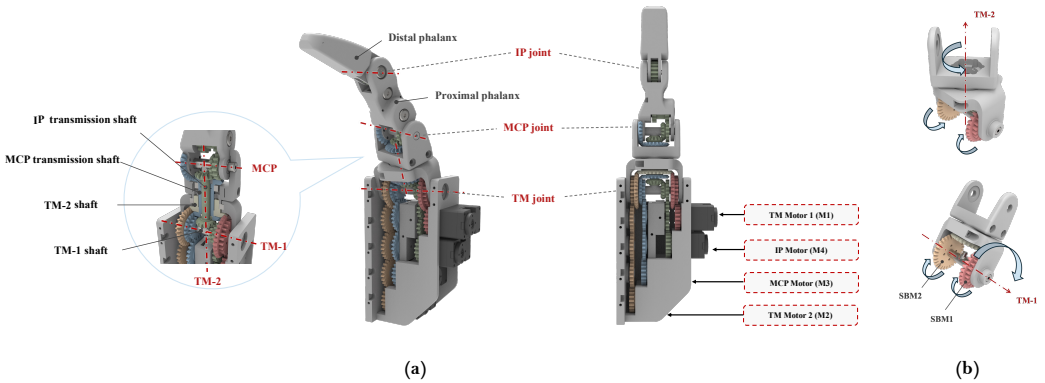

Figure 3: **Mechanical design of the thumb finger**. The red and orange sections represent the TM joint transmission gear set, the blue section the MCP gear set, and the green section the IP gear set.

2.3 Omnidirectional Thumb Actuation Mechanism

The thumb is designed with unique actuation requirements, distinct from the other fingers, to support its complex movements. Unlike the other fingers, the thumb requires multi-axis control for human-like motion, including flexion/extension, abduction/adduction, and rotation. To meet these demands, we introduce a novel **omnidirectional thumb actuation mechanism**, which integrates differential control for the TM joint and efficient transmission for the MCP and IP joints.

As illustrated in Fig. 3 (b), the TM joint offers two degrees of freedom: flexion/extension (TM-1) and abduction/adduction (TM-2), driven by two motors (M1 and M2). These motors operate through a differential mechanism, allowing independent and simultaneous control. M1 and M2 drive spur-bevel gear modules (SBM1 and SBM2), which engage the gear fixed on the TM-2 shaft. When SBM1 and SBM2 rotate at the same speed in the same direction, flexion/extension occurs. Opposite rotations at the same speed produce abduction/adduction. Compound motions are achieved by superimposing rotational speeds, enabling smooth omnidirectional thumb movements crucial for dexterous manipulation.

Transmission for the MCP and IP joints requires shifting gear axes from the TM-1 to TM-2 direction, then to the MCP/IP direction. To address this, a transmission shaft with bevel gears is embedded in the TM joint, as shown in Fig. 3 (a). The bevel gear at one end engages with an SBM on the TM-1 shaft, connected to the M3 motor. The other end engages a bevel gear on the proximal phalanx, coaxial with the MCP joint. The IP joint transmission is similarly structured, with a nested design of coaxial shafts for the MCP and IP joints.

3 EXPERIMENTAL VALIDATION

3.1 Quantitative Evaluation

Thumb Opposability Volume measures the thumb's ability to oppose other fingers, reflecting the spatial range where the thumb can make contact. The RAPID Hand shows significantly larger finger-to-thumb opposability volumes across all fingers compared to the Shadow Hand, with values of 229,705 mm³ for the index finger, 227,154 mm³ for the middle finger, 173,029 mm³ for the ring finger, and 65,861 mm³ for the pinky finger. In contrast, the Shadow Hand exhibits much smaller volumes, particularly for the pinky finger (25,515 mm³), indicating less flexibility. These results suggest that the RAPID Hand's optimized design, which avoids bulky finger components, enhances its dexterity, especially for non-prehensile manipulation tasks.

Manipulability Ellipsoid volume represents the ability of the fingertips to move in different directions, calculated from the hand's Jacobian [17]. In three different configurations—down, up, and curled—the Shadow Hand shows superior linear manipulability, with volumes of 2.19×10^5 mm³

Figure 4: **Illustrations of the teleoperation tasks.** (a) The robot retrieves an object from a densely stacked drawer using multi-fingered non-prehensile manipulation. (b) It picks up a ladle from a table and adjusts its pose for human-like use. (c) The robot plays a piano, mimicking a pianist's actions.

(down), 6.35×10^3 mm³ (up), and 2.29×10^5 mm³ (curled). The RAPID Hand's linear manipulability is lower, with 1.69×10^4 mm³ (down), 2.37×10^2 mm³ (up), and 1.46×10^5 mm³ (curled). Angular manipulability is also lower for the RAPID Hand (4.61 mm³ across all positions) compared to the Shadow Hand's angular values of 11.4 mm³ (down and curled) and 11.2 mm³ (up). These differences highlight areas where the RAPID Hand's design could be further refined to improve movement efficiency.

3.2 Qualitative Evaluation

To qualitatively evaluate the RAPID Hand's fully actuated 20-DoF design, we conducted teleoperation experiments using an Apple Vision Pro, testing the hand on three challenging tasks: multi-finger retrieval, ladle handling, and human-like piano playing.

Multi-finger retrieval. Unlike typical object retrieval tasks [18, 19, 20, 21] that rely on parallel grippers and arm motion, we design a scenario where the object is buried in a cluttered drawer, requiring non-prehensile, multi-finger manipulation. The RAPID Hand successfully retrieves the object, thanks to its thin fingers and palm-located motors, highlighting the importance of non-bulky finger design for such tasks (Fig. 4 (a)).

Ladle handling. This task involves picking up a ladle from a flat surface and adjusting its orientation in-hand using multi-finger manipulation. While the RAPID Hand grasps and manipulates the ladle, occasional failures occur due to difficulties in grasping the shank, which requires precise fingertip control (Fig. 4 (b)). This indicates that fully actuated hands have potential for complex in-hand manipulation but may need further refinement.

Human-like piano playing. In this task, the RAPID Hand plays an electronic piano, mimicking human performance with arm and finger movements. Though it completes the task, precision issues in hand pose tracking and finger sequencing affect performance (Fig. 4 (c)). These results show the potential of a fully actuated 20-DoF design for complex tasks and suggest room for improvement in control precision.

4 Conclusion

This paper presents the RAPID Hand, a low-cost, biomimetic dexterous hand with a novel actuation and transmission scheme. Experimental results show the value of its 20-DoA design, though improvements are needed. By open-sourcing the design, we aim to encourage innovation and collaboration in the robotics community. Future work will integrate tactile sensors for learning-based manipulation beyond teleoperation.

Acknowledgments

This research was supported by Orbot Ltd and partially by the National Natural Science Foundation of China under Grant 62173352.

References

[1] R. R. Ma and A. M. Dollar. On dexterity and dexterous manipulation. In *2011 15th International Conference on Advanced Robotics (ICAR)*, pages 1–7. IEEE, 2011.

[2] O. M. Andrychowicz, B. Baker, M. Chociej, R. Jozefowicz, B. McGrew, J. Pachocki, A. Petron, M. Plappert, G. Powell, A. Ray, et al. Learning dexterous in-hand manipulation. *The International Journal of Robotics Research*, 39(1):3–20, 2020.

[3] Y. Chen, C. Wang, L. Fei-Fei, and C. K. Liu. Sequential dexterity: Chaining dexterous policies for long-horizon manipulation. *arXiv preprint arXiv:2309.00987*, 2023.

[4] C. Chi, S. Feng, Y. Du, Z. Xu, E. Cousineau, B. Burchfiel, and S. Song. Diffusion policy: Visuomotor policy learning via action diffusion. In *Proceedings of Robotics: Science and Systems (RSS)*, 2023.

[5] H. Qi, B. Yi, S. Suresh, M. Lambeta, Y. Ma, R. Calandra, and J. Malik. General in-hand object rotation with vision and touch. In *Conference on Robot Learning*, pages 2549–2564. PMLR, 2023.

[6] T. Z. Zhao, V. Kumar, S. Levine, and C. Finn. Learning fine-grained bimanual manipulation with low-cost hardware. *arXiv preprint arXiv:2304.13705*, 2023.

[7] Z. Fu, T. Z. Zhao, and C. Finn. Mobile aloha: Learning bimanual mobile manipulation with low-cost whole-body teleoperation. *arXiv preprint arXiv:2401.02117*, 2024.

[8] C. Chi, Z. Xu, C. Pan, E. Cousineau, B. Burchfiel, S. Feng, R. Tedrake, and S. Song. Universal manipulation interface: In-the-wild robot teaching without in-the-wild robots. In *Proceedings of Robotics: Science and Systems (RSS)*, 2024.

[9] C. Wang, H. Shi, W. Wang, R. Zhang, L. Fei-Fei, and C. K. Liu. Dexcap: Scalable and portable mocap data collection system for dexterous manipulation. *arXiv preprint arXiv:2403.07788*, 2024.

[10] H. Fang, H.-S. Fang, Y. Wang, J. Ren, J. Chen, R. Zhang, W. Wang, and C. Lu. Airexo: Low-cost exoskeletons for learning whole-arm manipulation in the wild. In *2024 IEEE International Conference on Robotics and Automation (ICRA)*, pages 15031–15038. IEEE, 2024.

[11] Allegrohand. https://www.wonikrobotics.com/research-robot-hand. Accessed: 2024-10-06.

[12] Shadowhand. https://ninjatek.com/shop/edge/. Accessed: 2024-10-06.

[13] Inspirehand. https://inspire-robots.store. Accessed: 2024-10-06.

[14] K. Shaw, A. Agarwal, and D. Pathak. Leap hand: Low-cost, efficient, and anthropomorphic hand for robot learning. *arXiv preprint arXiv:2309.06440*, 2023.

[15] Abilityhand. https://www.psyonic.io/ability-hand. Accessed: 2024-10-06.

[16] I. Cerulo, F. Ficuciello, V. Lippiello, and B. Siciliano. Teleoperation of the schunk s5fh underactuated anthropomorphic hand using human hand motion tracking. *Robotics and Autonomous Systems*, 89:75–84, 2017.

[17] T. Yoshikawa. Manipulability of robotic mechanisms. *The international journal of Robotics Research*, 4(2):3–9, 1985.

[18] A. Zeng, S. Song, S. Welker, J. Lee, A. Rodriguez, and T. Funkhouser. Learning synergies between pushing and grasping with self-supervised deep reinforcement learning. In *2018 IEEE/RSJ International Conference on Intelligent Robots and Systems (IROS)*, pages 4238–4245. IEEE, 2018.

[19] B. Tang, M. Corsaro, G. Konidaris, S. Nikolaidis, and S. Tellex. Learning collaborative pushing and grasping policies in dense clutter. In *2021 IEEE International Conference on Robotics and Automation (ICRA)*, pages 6177–6184. IEEE, 2021.

[20] Y. Yang, Z. Ni, M. Gao, J. Zhang, and D. Tao. Collaborative pushing and grasping of tightly stacked objects via deep reinforcement learning. *IEEE/CAA Journal of Automatica Sinica*, 9 (1):135–145, 2021.

[21] J. Xu, Y. Jia, D. Yang, P. Meng, X. Zhu, Z. Guo, S. Song, and M. Ciocarlie. Tactile-based object retrieval from granular media. *arXiv preprint arXiv:2402.04536*, 2023.